

## Smallest Carbon Nanotube Is 3 Å in Diameter

X. Zhao,<sup>1,\*</sup> Y. Liu,<sup>2</sup> S. Inoue,<sup>1</sup> T. Suzuki,<sup>1</sup> R. O. Jones,<sup>2</sup> and Y. Ando<sup>1</sup>

<sup>1</sup>Department of Materials Science and Engineering, 21st Century COE Program "Nano Factory," Meijo University, Nagoya 468-8502, Japan

<sup>2</sup>Institut für Festkörperforschung, Forschungszentrum Jülich, D-52425 Jülich, Germany

(Received 21 August 2003; published 23 March 2004)

Previous energetic considerations have led to the belief that carbon nanotubes (CNTs) of 4 Å in diameter are the smallest stable CNTs. Using high-resolution transmission electron microscopy, we find that a stable 3 Å CNT can be grown inside a multiwalled carbon nanotube. Density functional calculations indicate that the 3 Å CNT is the armchair CNT(2,2) with a radial breathing mode at 787 cm<sup>-1</sup>. Each end can be capped by half of a C<sub>12</sub> cage (hexagonal prism) containing tetragons.

DOI: 10.1103/PhysRevLett.92.125502

PACS numbers: 61.46.+w, 61.50.Ah, 81.07.De

Previous energetic considerations [1] have indicated that 4 Å is the smallest possible diameter of carbon nanotubes (CNTs), and the 4 Å CNTs [2,3] can be capped with a hemisphere of the smallest fullerene C<sub>20</sub> containing only pentagons [4]. Another calculation [5] predicts that some sub-4 Å CNTs could be mechanically stable at temperatures as high as 1100 °C. It is natural to ask: what is the smallest possible CNT? We report the discovery by high-resolution transmission electron microscopy (HRTEM) of the smallest stable 3 Å CNT, which is formed inside a multiwalled carbon nanotube (MWNT) prepared by hydrogen arc discharge [6]. Density functional calculations show that the 3 Å CNT is probably the armchair CNT(2,2), and each end can be capped by half of a C<sub>12</sub> cage [7] that includes pentagons and tetragons. The calculated frequency of a radial breathing mode (RBM) for the CNT(2,2) is around 787 cm<sup>-1</sup>, so that Raman spectroscopy should also be able to demonstrate the existence of a 3 Å diameter nanotube.

The physical properties of CNTs depend on their diameter and chirality. Sub-5 Å CNTs tend to be metallic due to strong  $\sigma^*-\pi^*$  hybridization resulting from severe tube curvature [8], and 4 Å CNTs have been found to be superconducting [9]. Using an arc discharge with hydrogen [6] instead of helium [10], Qin *et al.* have prepared 4 Å CNTs confined inside MWNTs [2]. Moreover, a new one-dimensional (1D) carbon allotrope, the carbon nanowire (CNW), consisting of a long linear carbon chain inserted into the innermost tube of an MWNT, has also been found [11]. The same preparation method [2,6,11] has been used here in pure hydrogen gas at a pressure of  $8.0 \times 10^3$  Pa. For HRTEM observations (JEOL-2010F, at 120 kV), the core of the cathode deposit including MWNTs was ground to fine powder in ethanol, dispersed ultrasonically, and placed on a TEM microgrid.

Figure 1 shows a typical HRTEM image of the 3 Å CNT formed inside an MWNT. This 3 Å CNT has a length of 140 Å and has a carbon cap at each end, marked by horizontal arrows, A and A'. The diameter of the 3 Å CNT is much smaller than the interlayer spacing of the

MWNT, 3.4 Å (both are indicated by a pair of lines marked by arrows). *Scion image*, an image processing and analysis program, has been used to analyze the HRTEM image and to measure accurately the diameter of the 3 Å CNT. An image contrast profile (Scion image) across the MWNT at the position marked by two vertical arrows (B and B' in Fig. 1) is shown in the lower right inset of Fig. 2. The weak pair of peaks (0, 0') originates from the 3 Å CNT, and the strong pair (1, 1') comes from the innermost tube in the MWNT. The unusually high contrast results from the local structure distortion caused by the strong attraction between the 3 Å CNT and the innermost tube in the MWNT.

The MWNT consists of 12 concentric CNTs with progressively increasing diameters and constant interlayer spacings. Using the value [12] of interlayer spacing, 3.4 Å, as a calibration standard, we have measured the diameter of the 3 Å CNT and all other CNTs in the MWNT. The results are plotted as a function of the number of CNTs in the MWNT in Fig. 2, where

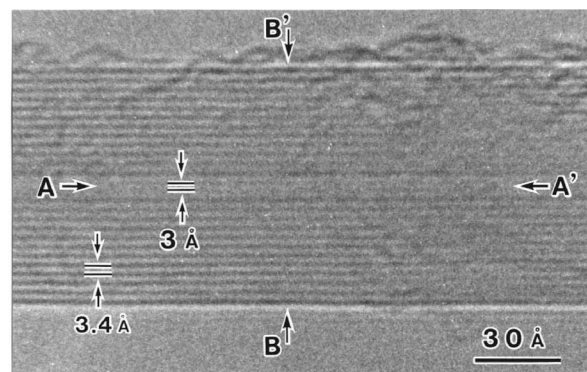


FIG. 1. HRTEM image of 3 Å CNT formed inside MWNT. The diameter of 3 Å CNT and the interlayer space of MWNT, 3.4 Å, are indicated by a pair of lines marked by arrows. Each end is marked by two horizontal arrows, A and A'. The diameter of the 3 Å CNT is much smaller than the interlayer spacing of the

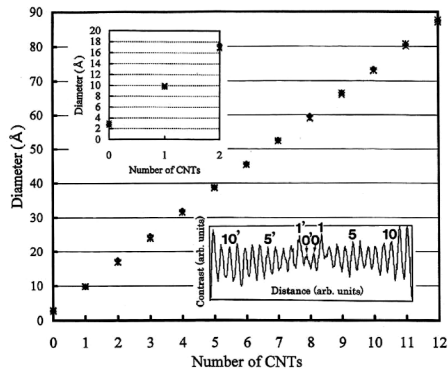


FIG. 2. Diameter of 3 Å CNT, and the diameters of CNTs in MWNT plotted as a function of the number of CNTs in MWNT. Diameters of 3 Å CNT, the innermost tube in MWNT, and the second CNT in MWNT are shown in the upper left inset. The lower right inset is an image contrast profile across the MWNT at the position marked by two vertical arrows,  $B$  and  $B'$ , in Fig. 1.

0 corresponds to the 3 Å CNT, 1 to the innermost tube in the MWNT, and 12 to the outermost tube. The data, indicated by the symbols (\*, +, ◆), came from three image contrast profiles obtained from three different positions (one is marked by  $B-B'$  in Fig. 1, and the other two are located 40 Å apart on both sides). The magnified data of diameters of the 3 Å CNT (number of CNTs, 0), the innermost tube in the MWNT (number of CNTs, 1), and the second CNT in the MWNT (number of CNTs, 2) are shown in the upper left inset of Fig. 2. These data can be fitted well to a straight line due to the constant inter-layer spacing of the MWNT, and they show that the CNTs in the MWNT have uniform diameters. The average of three measurements leads to our estimate of the diameter of the smallest nanotube as 2.8 Å. The diameters of the innermost and outermost tubes in the MWNT are 9.8 and 87.4 Å, respectively.

A CNT can be regarded as a graphitic cylinder generated by rolling one sheet of graphite, “graphene.” If the C-C bond length in graphene is 1.42 Å, there are three possible CNT structures for the 3 Å CNT: the zigzag CNT(4, 0), the armchair CNT(2, 2), and the chiral CNT(3, 1) with unrelaxed diameters of 3.32, 2.72, and 2.83 Å, respectively.

We have performed density functional calculations with simulated annealing [13] to study the structures of these three CNTs. The optimized diameters have been obtained by using infinitely long tubes obtained by applying periodic boundary conditions along the axis of the CNT, e.g., for the open-ended model of CNT(2, 2) in Fig. 3(a). The CNT(2, 2) has the smallest diameter (2.81 Å), followed by CNT(3, 1) (3.03 Å) and CNT(4, 0) (3.32 Å). The method is described in detail elsewhere [14]. The energy differences are relatively small, with the largest CNT(4, 0) being 0.15 eV/atom more stable than CNT(3, 1), with CNT(2, 2) an additional

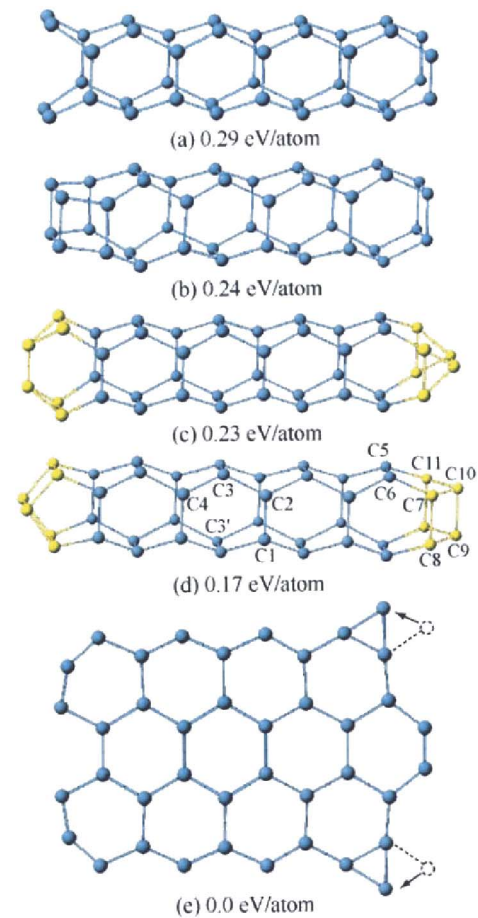


FIG. 3 (color online). Supercell models of isolated CNT(2, 2) and graphene strip. (a) “Open-ended” model with total energy of 0.29 eV/atom. (b) “Closed” model, 0.24 eV/atom. (c) “Triangle cap-ended” model, 0.23 eV/atom. (d) “Square cap-ended” model, 0.17 eV/atom. (e) Graphene strip obtained by unrolling CNT(2, 2), 0.0 eV/atom as reference.

0.12 eV/atom higher in energy. The smaller CNT have diameters larger than the unrelaxed structures, as noted previously [14–19], and the dilation can be more than 3% in CNT with diameters less than 4 Å [14,16–19]. Our calculations are consistent with these findings, and they show that CNT(2, 2) is the only structure that is consistent with the diameter measured in HRTEM (2.8 Å). Note that the further radial expansion of 3 Å CNT induced by the innermost tube in MWNT [e.g., CNT(2, 2)@(7, 7) in Ref. [14]] make the other two structures more unlikely. The temperature at which the CNT are produced is so high that the small differences in the total energy play a little role.

These calculations have been extended to study the energetics and geometries of CNT(2, 2) with caps at each end. Four supercell models of isolated CNT(2, 2) segments, whose geometries have been optimized using simulated annealing [13], are shown in Figs. 3(a)–3(d). A supercell model of a graphene strip obtained by unrolling

TABLE I. Structural parameters of CNT(2, 2) cap in the square cap-ended model.

C-C bond length (Å)		Bond angle	
$L_{C5C6}$	1.43	$\theta_{C5C6C7}$	107.0°
$L_{C6C7}$	1.46	$\theta_{C6C7C8}$	109.2°
$L_{C7C8}$	1.52	$\theta_{C6C7C10}$	109.2°
$L_{C8C9}$	1.45	$\theta_{C7C10C11}$	103.8°
$L_{C9C10}$	1.47	$\theta_{C7C8C9}$	89.0°
$L_{C8C11}$	2.74	$\theta_{C8C9C10}$	91.0°

the CNT(2, 2) is depicted in Fig. 3(e). The total energy of this graphene strip defines the zero of energy used in the following discussion.

The “open-ended” model [Fig. 3(a)], the “closed” model [Fig. 3(b)], and the “triangle cap-ended” model [Fig. 3(c)] have total energies of 0.29, 0.24, and 0.23 eV/atom. The “square cap-ended” model [Fig. 3(d)] has the lowest total energy (0.17 eV/atom) among the CNT(2, 2) models. In Table I, the structural parameters of the CNT(2, 2) cap in the square cap-ended model are presented. We note that the pentagons have a torsion angle  $\theta_{C5C6C7C10} = 12.0^\circ$ . As the CNT diameter is reduced to 3 Å, it is essential to introduce two tetragons to form a cap structure [see Fig. 3(d)], which can be viewed as half of a  $C_{12}$  cage, a hexagonal prism [7].

For the infinite CNT(2, 2), which has four hexagons around its circumference, severe steric distortion from the graphitic  $sp^2$  bond takes place. The C-C bond perpendicular to the tube axis,  $L_{C1C2}$  [see Fig. 3(d)], is shortened to 1.38 Å, whereas the other bond,  $L_{C2C3}$ , is elongated to 1.50 Å. Moreover, although one of the bond angles ( $\theta_{C2C3C4} = 119.7^\circ$ ) remains near the graphitic  $sp^2$  bond angle of  $120^\circ$ , the other decreases to  $\theta_{C1C2C3} = 110.8^\circ$  [see Fig. 3(d)] near the tetrahedral  $sp^3$  bond angle of  $109.5^\circ$ .

Raman spectroscopy could also be used to confirm the existence of the 3 Å CNT formed inside the MWNT, by using established techniques for studying the Raman spectra of the MWNT and the RBM of the 4 Å CNT confined inside the MWNT [20,21]. The Raman spectrum of the infinite CNT(2, 2) was calculated using a finite difference method [13]. The RBM frequency is predicted to be about  $787 \text{ cm}^{-1}$ , the detection of which would require the use of resonance Raman enhancement effects. Since the Kataura plot [22] cannot be used to predict the resonance conditions, electronic structure calculations should be performed for the CNT(2, 2) before attempting to observe its RBM.

The total energy of the infinite CNT(2, 2) lies 0.27 eV/atom above that of the corresponding graphene strip and deviates slightly from the relative energy calculated by the open-ended model of the finite CNT(2, 2)

(0.29 eV/atom). This shows that the CNT(2, 2) has a higher energy than the corresponding graphene strip, in good agreement with previous predictions [1,5,19]. The growth mechanism of the 3 Å CNTs should be similar to that of the 4 Å CNTs confined inside MWNTs [2] and CNWs [11]. Both hydrogen atoms and very high temperature produced by the arc plasma play an important role in the formation of the 3 Å CNTs. It remains a challenge to prepare 3 Å CNTs in the channels of a porous zeolite crystal, or in single-wall carbon nanotubes with diameters of approximately 10 Å.

We thank the Forschungszentrum Jülich, Germany and the John von Neumann Institute for Computing (NIC) for generous access to the Cray T3E supercomputers in the FZ Jülich, and the Research Center for Computational Science (RCCS) at the Okazaki National Research Institute, Japan, for a grant of computer time on the Fujitsu VPP5000 supercomputers in Okazaki.

\*To whom correspondence should be addressed.

Electronic address: zhao@ccmfs.meijo-u.ac.jp

- [1] S. Sawada and N. Hamada, Solid State Commun. **83**, 917 (1992).
- [2] L.-C. Qin *et al.*, Nature (London) **408**, 50 (2000).
- [3] N. Wang, Z. K. Tang, G. D. Li, and J. S. Chen, Nature (London) **408**, 50 (2000).
- [4] H. Prinzbach *et al.*, Nature (London) **407**, 60 (2000).
- [5] L.-M. Peng *et al.*, Phys. Rev. Lett. **85**, 3249 (2000).
- [6] X. Zhao *et al.*, Carbon **35**, 775 (1997).
- [7] R. O. Jones, J. Chem. Phys. **110**, 5189 (1999).
- [8] X. Blase, L. X. Benedict, E. L. Shirley, and S. G. Louie, Phys. Rev. Lett. **72**, 1878 (1994).
- [9] Z. K. Tang *et al.*, Science **292**, 2462 (2001).
- [10] T. W. Ebbesen and P. M. Ajayan, Nature (London) **358**, 220 (1992).
- [11] X. Zhao, Y. Ando, Y. Liu, M. Jinno, and T. Suzuki, Phys. Rev. Lett. **90**, 187401 (2003).
- [12] S. Iijima, Nature (London) **354**, 56 (1991).
- [13] J. Hutter *et al.*, CPMD Program, version 3.5. IBM Corp. (1990–2001) and MPI für Festkörperforschung, Stuttgart, Germany (1997–2001).
- [14] Y. Liu, R. O. Jones, X. Zhao, and Y. Ando, Phys. Rev. B **68**, 125413 (2003).
- [15] D. Sánchez-Portal, E. Artacho, J. M. Soler, A. Rubio, and P. Ordejón, Phys. Rev. B **59**, 12 678 (1999).
- [16] K. Kanamitsu and S. Saito, J. Phys. Soc. Jpn. **71**, 483 (2002).
- [17] N. Sano, M. Chhowalla, D. Roy, and G. A. J. Amaratunga, Phys. Rev. B **66**, 113403 (2002).
- [18] H. J. Liu and C. T. Chan, Phys. Rev. B **66**, 115416 (2002).
- [19] I. Cabria, J. W. Mintmire, and C. T. White, Phys. Rev. B **67**, 121406 (2003).
- [20] X. Zhao *et al.*, Appl. Phys. Lett. **81**, 2550 (2002).
- [21] X. Zhao *et al.*, Chem. Phys. Lett. **361**, 169 (2002).
- [22] H. Kataura *et al.*, Synth. Met. **103**, 2555 (1999).